Free Radical Biology and Medicine 97 (2016) 95–108

Contents lists available at ScienceDirect

Free Radical Biology and Medicine

journal homepage: www.elsevier.com/locate/freeradbiomed

Evaluation of NADPH oxidases as drug targets in a mouse model of familial amyotrophic lateral sclerosis

Tamara Seredenina [a], Zeynab Nayernia [a], Silvia Sorce [b], Ghassan J. Maghzal [c,d], Aleksandra Filippova [a], Shuo-Chien Ling [e,f,g], Olivier Basset [a], Olivier Plastre [a], Youssef Daali [h], Elisabeth J. Rushing [b], Maria T. Giordana [i], Don W. Cleveland [e,f], Adriano Aguzzi [b], Roland Stocker [c,d], Karl-Heinz Krause [a,j], Vincent Jaquet [a,*]

[a] Department of Pathology and Immunology, Medical School, University of Geneva, Switzerland
[b] Institute of Neuropathology, University Hospital of Zurich, Zurich, Switzerland
[c] Victor Chang Cardiac Research Institute, Vascular Biology Division, 405 Liverpool Street, Darlinghurst, NSW 2010, Australia
[d] School of Medical Sciences, Faculty of Medicine, University of New South Wales, NSW 2052, Australia
[e] Ludwig Institute for Cancer Research, University of California, San Diego, La Jolla, CA 92093, USA
[f] Department of Cellular and Molecular Medicine, University of California, San Diego, La Jolla, CA 92093, USA
[g] Department of Physiology, National University of Singapore, Singapore
[h] Division of Clinical Pharmacology and Toxicology, Geneva University Hospital, Geneva, Switzerland
[i] Department of Neuroscience, Medical School of the University of Turin, Italy
[j] Department of Genetic and Laboratory Medicine, Geneva University Hospitals, Switzerland

ARTICLE INFO

Article history:
Received 11 March 2016
Received in revised form
29 April 2016
Accepted 17 May 2016
Available online 19 May 2016

Keywords:
NADPH oxidase
NOX
Amyotrophic lateral sclerosis
Microglia
Phenothiazine
Perphenazine
Thioridazine
SOD1^{G93A} mice

ABSTRACT

Amyotrophic lateral sclerosis (ALS) is an incurable neurodegenerative disease characterized by progressive loss of motor neurons, gliosis, neuroinflammation and oxidative stress. The aim of this study was to evaluate the involvement of NADPH oxidases (NOX) in the oxidative damage and progression of ALS neuropathology. We examined the pattern of NOX expression in spinal cords of patients and mouse models of ALS and analyzed the impact of genetic deletion of the NOX1 and 2 isoforms as well as pharmacological NOX inhibition in the SOD1^{G93A} ALS mouse model.

A substantial (10–60 times) increase of NOX2 expression was detected in three etiologically different ALS mouse models while up-regulation of some other NOX isoforms was model-specific. In human spinal cord samples, high NOX2 expression was detected in microglia. In contrast to previous publications, survival of SOD1^{G93A} mice was not modified upon breeding with constitutive NOX1 and NOX2 deficient mice. As genetic deficiency of a single NOX isoform is not necessarily predictive of a pharmacological intervention, we treated SOD1^{G93A} mice with broad-spectrum NOX inhibitors perphenazine and thioridazine. Both compounds reached *in vivo* CNS concentrations compatible with NOX inhibition and thioridazine significantly decreased superoxide levels in the spinal cord of SOD1^{G93A} mice *in vivo*. Yet, neither perphenazine nor thioridazine prolonged survival. Thioridazine, but not perphenazine, dampened the increase of microglia markers in SOD1^{G93A} mice. Thioridazine induced an immediate and temporary enhancement of motor performance (rotarod) but its precise mode of action needs further investigation. Additional studies using specific NOX inhibitors will provide further evidence on the relevance of NOX as drug targets for ALS and other neurodegenerative disorders.

List of abbreviations: ALS, amyotrophic lateral sclerosis; BBB, blood brain barrier; 2-Cl-E$^+$, 2-chloroethidium; CNS, central nervous system; DMSO, Dimethylsulfoxide; DPI, diphenyleneiodonium; DMEM, Dulbecco's modified Eagle Medium; DNA, deoxyribonucleic acid; DUOX, dual oxidase; E$^+$, ethidium; EC_{50}, half maximal efficient concentration; FBS, fetal bovine serum; FUS/TLS, Fused in Sarcoma/Translocated in Sarcoma; GM-CSF, granulocyte-macrophage colony-stimulating factor; HBSS, Hank's buffered salt solution; HE, hydroethidine; HOCl, hypochlorous acid; H_2O_2, hydrogen peroxide; 2-OH-E$^+$, 2-hydroxyethidium; LC/MS/MS, Liquid chromatography-tandem mass spectrometry; MPO, myeloperoxidase; NADPH, nicotinamide adenine dinucleotide phosphate; NOX, NADPH oxidase; NOXO1, NADPH oxidase organiser type 1; NC, non-carrier; PBS, phosphate buffered saline; PMA, phorbol myristate acetate; qPCR, quantitative polymerase chain reaction; ROS, reactive oxygen species; $O_2^{\bullet-}$, superoxide radical anion; SOD, superoxide dismutase; TDP 43, TAR DNA binding protein 43; WST-1, 2-(4-Iodophenyl)-3-(4-nitrophenyl)-5-(2,4-disulfophenyl)-2H-tetrazolium, monosodium salt; WT, wild type

* Corresponding author.
E-mail address: Vincent.Jaquet@unige.ch (V. Jaquet).

http://dx.doi.org/10.1016/j.freeradbiomed.2016.05.016

1. Introduction

Amyotrophic lateral sclerosis (ALS) is a disease leading to motor neuron degeneration, paralysis and death usually within five years following diagnosis. Currently there is no cure for ALS. New therapies and identification of novel pharmacological targets are urgently needed. The etiology of the disease appears multiple, but remains unclear for most cases. A strong neuroinflammation in the brain stem and spinal cord parenchyma is believed to contribute to ALS progression. At the pathological level, neuroinflammation is characterized by the proliferation and activation of microglia and astrocytes, accompanied by the invasion of the central nervous system (CNS) parenchyma by inflammatory cells. Although neuroinflammation may be neuroprotective in some instances, excessive production of pro-inflammatory cytokines and reactive oxygen species (ROS) is believed to contribute to disease progression [1].

ROS are important signaling molecules necessary for a range of physiological processes. However, excessive production of ROS causes damage of biomolecules interfering with their normal functions and leading ultimately to cellular dysfunction or even death. A major source of ROS in the CNS is the family of NADPH oxidases (NOX) [2]. NOX are transmembrane proteins comprising 7 members (NOX1-NOX5, DUOX1 and DUOX2), each with a specific tissue distribution and activation mechanism [3]. NOX catalyze the reduction of molecular oxygen to superoxide radical anion ($O_2^{\bullet -}$), which in turn can give rise to other ROS, such as hydrogen peroxide (H_2O_2) and hypochlorous acid (HOCl) [4]. Recent studies have shown that genetic deletion of NOX isoforms is neuroprotective in mouse models of Parkinson's disease [5], stroke [6], and prion disease [7]. Previous studies have proposed NOX1 and NOX2 as potential drug targets since they contribute to disease progression in a mouse model of ALS [8,9]. Moreover, it was recently shown that NOX2 activity in peripheral neutrophils of ALS patients has a prognosis value for disease outcome as lower NOX2 activity correlated with increased survival [9].

However, the therapeutic relevance of NOX inhibition remains unclear as validated specific small molecule NOX inhibitors are only emerging [10,11]. We have recently found that some N-substituted members of the phenothiazine family inhibit NOX isoforms 1–5 [12]. Phenothiazines have numerous pharmacological properties [13], and are used in humans as antipsychotics and antiemetics. Since they cross the blood-brain barrier (BBB), we hypothesized that they may inhibit NOX activity in ALS spinal cord, curb neuroinflammation and slow down the progression of the disease. To test this hypothesis, we administered perphenazine or thioridazine to $SOD1^{G93A}$ mice, a model of familial ALS, and evaluated the effect on clinical symptoms and molecular markers of the disease.

2. Methods

2.1. Chemicals and reagents

Hank's buffered salt solution (HBSS), fetal bovine serum (FBS) and Amplex Red were purchased from Invitrogen. Thioridazine hydrochloride, perphenazine, penicillin, streptomycin, phorbol myristate acetate (PMA), diphenylene iodonium chloride (DPI), dimethyl sulfoxide, superoxide dismutase 1 bovine (Cu/Zn SOD1), catalase and Tween-20 were purchased from Sigma Aldrich. 2-(4-Iodophenyl)-3-(4-nitrophenyl)-5-(2,4-disulfophenyl)-2H-tetrazolium, monosodium salt (WST-1) was acquired from Dojindo Molecular Technologies.

2.2. RA2 Cells

The granulocyte macrophage colony-stimulating factor (GM-CSF)-dependent Ra2 microglia cell line generated by spontaneous immortalization of primary mouse microglia [14] was cultured in minimal essential medium with 10% fetal calf serum, 8 ng/ml GM-CSF, penicillin (100 U/ml) and streptomycin (100 μg/ml) at 37 °C and 5% CO_2. RA2 cells were plated in 96 well plates at a density of 10000 cells/well and treated with 5 μg/ml LPS (ALX-581-007-L002, Enzo Life Sciences) 24 h after plating for additional 24 h.

2.3. ROS measurements in intact cells

Levels of H_2O_2 produced by intact cells were measured using Amplex Red fluorescence as described [15]. The concentration of $O_2^{\bullet -}$ was measured as absorbance change of 1 mM WST-1 at 440 nm [16]. Fluorescence and absorbance were measured in a FluoSTAR OPTIMA, BMG labtech instrument at 37 °C. Under the conditions of pre-treatment with LPS and stimulation with PMA, macrophages produce peroxynitrite [17], which can generate fluorescence in the HRP/Amplex red system [18]. The signal measured in microglial RA2 cells upon PMA stimulation is specific for H_2O_2 and $O_2^{\bullet -}$ as it is inhibited in a concentration-dependent manner by catalase in Amplex assay and by SOD in WST1 assay (Supplementary Fig 1).

2.4. Real-time quantitative polymerase chain reaction

RNA was extracted from mouse spinal cords ($SOD1^{G93A}$ mice), total brain (TDP43 and FUS mice) or from RA2 cells using the Qiagen RNeasy mini kit following the manufacturer's instructions. RNA concentration was determined using Nanodrop. 500 ng was used for cDNA synthesis using Takara PrimeScript RT reagent Kit following manufacturer's instruction. Real-time PCR was performed using SYBR green assay on a 7900HT SDS systems from ABI at the Genomics Platform, National Center of Competence in Research Frontiers in Genetics, Geneva. The efficiency of each primer was verified with serial dilutions of cDNA. Relative expression levels were calculated by normalization to geometric mean of the two house-keeping genes HPRT and GAPDH, as described previously [19]. The highest normalized relative quantity was arbitrarily designated as a value of 1.0. Fold changes were calculated from the quotient of means of these normalized quantities and reported as ± SEM. Sequences of all primers used in this study are provided in Supplementary Table 1. Threshold cycle (Ct) values for NOX subunits corresponding to the intersection between an amplification curve and a threshold line set at 0.20 by the software are provided in Supplementary Table 2.

2.5. Thioridazine and perphenazine determination in brain

Perphenazine (3 mg/kg) or thioridazine (10 mg/kg) were administered i.p. After a desired time period (30 min – 8 h) mice were sacrificed by lethal injection of Nembutal and perfused with 0.9% saline solution intracardially for 5 min. Brains were dissected, snap frozen in liquid nitrogen, and stored at −80°C. Brains were weighted and homogenized in 2 ml of deionized water. The final volume was adjusted to 5 mL with water. To 500 μL of homogenate, 100 μL of desmethylclobazam-d5 (internal standard) at 10 ng/mL and 3 mL of hexane/ethyl acetate (50/50 mixture) were added. Liquid-liquid extraction was performed by shaking samples for 30 min. After centrifugation at 1000 g for 10 min, the supernatant was removed, evaporated and the residue reconstituted in 200 μL of MeOH/water (1:1, v/v). Finally, 20 μL were injected onto the HPLC system. Along with the unknown samples, QC and standards samples, prepared using blank brain spiked with

thioridazine and perphenazine, covering the expected concentration range were processed. All experiments were performed using an API 4000 triple quadrupole mass spectrometer (AB Sciex, Concord, ON, Canada) controlled by Analyst 1.5.1 software. The mass spectrometer was operated in the multiple reaction monitoring (MRM) mode with positive electrospray ionization. The MRM transitions were 371.1→126.1, 404.1→171.1 and 292.1→249.8 with a dwell time of 50 ms for thioridazine, perphenazine and IS (desmethylclobazam-d5), respectively. The instrument was directly coupled to an Agilent series 1100 (Waldbronn, Germany) LC system. Chromatography was performed on a Phenomenex Kinetex C18 analytical column (50 mm × 2.1 mm, 2.6 μm; Torrance, CA, USA) preceded by a pre-column with the same phase. Flow rate was 0.5 mL/min using gradient elution conditions. The method was fully validated before application to this study. The concentration of drugs was normalized to brain tissue weight and expressed in μg/μl brain tissue assuming a brain density of 1.04 g/mL [20]. The normalization to volume was needed for the presentation of the IC50 values for phenothiaizine compounds (μg/μl) on the same graph.

2.6. In vivo labelling with dihydroethidium (HE) and detection of reactive species by LC/MS/MS

HE stock solution (25 mg/ml) was prepared on the day of the experiment in argon-purged DMSO under an argon-enriched atmosphere and with protection from light. 7.5 μl of this solution was mixed with 7.5 μl 0.9% NaCl and injected intraspinally into $SOD1^{G93A}$ mice (110 days). After 30 min mice were anesthetized with Nembutal and perfused intracardially for 5 min with 0.9% saline. Spinal cord was dissected, snap frozen and stored at −80 °C. Products of HE oxidation were quantified using LC/MS/MS analysis as described previously [21].

2.7. Western blotting

Protein extracts were prepared by lysing the spinal cord tissue in the buffer containing: 50 mM Tris–HCl pH 7.4; 50 mM NaCl; 10 mM MgCl2; 1 mM EGTA; 1% Triton-X100; Protease inhibitors (Roche). BioRad assay was used for protein quantification. Equal amount (30 μg) of protein was loaded for analysis. After transfer, the membrane was blocked for 1 h at room temperature in PBS/0.5% Tween-20 buffer containing 5% fat-free milk (blocking buffer). The membrane was incubated at 4 °C overnight with $gp91^{phox}$ antibody (BD Transduction Laboratories, BD611415; 1/500 diluted in blocking buffer). After washing, the membrane was incubated for 1 h at room temperature with horseradish peroxidase-conjugated secondary antibody (1/10,000 in blocking buffer). Unbound secondary antibody was washed off. ECL kit (GE Healthcare) was used to detect the signal.

2.8. Immunohistochemistry

Mice were anesthetized with Nembutal (i.p) and perfused intracardially with cold PBS followed by cold 4% paraformaldehyde (Sigma Aldrich, Saint Louis, USA). Spinal cords were removed and stored for 24 h in 4% paraformaldehyde. Lumbar sections were embedded in paraffin, cut in 10-μm-thick sections, and mounted on glass slides. Deparaffinization was performed by a gradient of alcohols. In order to expose the epitopes, tissues were boiled in citrate buffer (0.01 mol/L, pH=6) for 15 min. Prior to addition of antibodies, unspecific binding was prevented by incubation of tissues in blocking solution (0.2% Triton-X, 10% fetal calf serum, PBS) for 30 min. Incubation overnight was performed at 4 °C with either rabbit polyclonal Iba1 (Wako, 1:500) or mouse monoclonal glial fibrillary acidic protein (GFAP; MAB360, Chemicon, 1:1000) diluted in buffer (0.2% Triton-X100, PBS). Tissues were incubated with secondary antibodies Alexa Fluor (A21424 and A11034, Invitrogen, 1:1000) for 30 min, DAPI for 10 min and mounted with FluorSave (Calbiochem, San Diego). For visualization of neurons, tissues were deparaffinized, stained with 0.1% cresyl violet for 5 min, and then dehydrated by a gradient of alcohols. Technical controls were performed for each experiment by omitting the first antibody and performing the other steps of the procedure (data not shown). Motor neurons were counted manually in the anterior horn of mouse spinal cord slices. The intensity of Iba1 and GFAP staining was analyzed using ImageJ software.

Table 1
Basic characteristics of ALS and non-ALS control patients.

Patient no	Gender	Age at death (years)	Duration of disease (months)	Pathology
1	F	67	14	ALS
2	F	60	30	ALS
3	M	46	72	ALS
4	M	77	19	ALS
5	F	62	n. a.	ALS
6	M	77	30	ALS
C1	M	72	–	Atrial fibrillation; leptomeningeal venous angioma of the cervical spinal cord
C2	M	36	–	Gliomatosis cerebri
C3	F	73	–	Central pontine myelinolysis

n. a.=not available

2.9. Immunostaining in human tissues

2.9.1. Patients

Human tissue samples used in this study (Table 1) were obtained from the archive of the Institute of Neuropathology, University Hospital Zurich (samples 4–6, C3) and from the archive of the Laboratory of Neuropathology, Department of Neuroscience, University of Turin (samples 1–3, C1–C2). Samples were irreversibly anonymized, dated prior to the year 2005, processed and analyzed according to the Swiss Medical-ethical guidelines and recommendations (Senate of the Swiss Academy of Medical Sciences, Basel, Switzerland, 23 May 2006).

2.9.2. Immunohistochemistry

NOX2 staining was performed as described in [7]. Briefly, anti-human NOX2 (1:250, Clone 48, Sanquin) antibody was applied to sections after deparaffinization and antigen retrieval. Staining was visualized using DAB (Sigma-Aldrich) and H_2O_2 (Sigma-Aldrich), after incubation with a biotinylated secondary antibody (Vector Laboratories) and the ABC complex solution (Vector laboratories). Hematoxylin counterstain was subsequently performed. Quantification of NOX2 expression in spinal cord sections was performed as described before [7] on regions of interest drawn on different areas of spinal cord sections.

2.10. Animals used in the study

B6SJL-Tg($SOD1^{G93A}$)1Gur/J (Stock Number: 002726) [22] mice were purchased from Jackson laboratory and kept in standard conditions in the conventional animal facility of Centre Médical Universitaire of the University of Geneva with free access to food and water. All experiments were approved by the local veterinary office and the Commission for Animal Experimentation of the Canton of Geneva, Switzerland, authorization number 1005/3445/2-R.

To generate ALS mice deficient for NOX2, B6SJL-Tg ($SOD1^{G93A}$)1Gur/J males were crossed with homozygous NOX2KO

B6.129S6-*Cybb*^{tm1Din}/J females (Jackson labs). From this breeding, NOX2-deficient males carrying the SOD1^{G93A} transgene were crossed to female non-carriers heterozygous for NOX2 deletion (NOX2$^{+/-}$). From this breeding, only the progeny carrying the SOD1^{G93A} transgene was used for survival analysis: for females NOX2$^{+/-}$/SOD Tg and NOX2$^{-/-}$/SOD Tg; for males NOX2$^{+/y}$/SOD Tg andNOX2$^{-/y}$/SOD Tg. Genotyping was performed following the Jackson lab protocols for B6SJL-Tg(SOD1^{G93A})1Gur/J and NOX2KO B6.129S6-*Cybb*^{tm1Din}/J.

RNA samples were obtained from symptomatic TDP-43 [23] and FUS [24] transgenic mice, in which broad CNS expression of human TDP-43 or FUS cDNA that mimic the endogenous TDP-43 and FUS expression pattern. In these two models, TDP-43 [23] or FUS/TLS [24] cDNA were placed under the control of a mouse prion promoter to achieve CNS expression patterns similar to those of endogenous TDP-43 and FUS/TLS. Mice expressing human TDP-43^{Q331K}, but not wild type human TDP-43, develop age-dependent loss of motor neurons by 12-month [21]. Heterozygous FUS/TLS^{WT} mice develop normally while the homozygous FUS/TLS^{WT} mice develop rapid and progressive neurological phenotypes leading to paralytic disease by 40 days of age (this new mouse model will be described in details elsewhere).

2.11. SOD1^{G93A} mice treatment

Litters were split to enable even distribution of parentage between the two comparison groups, and the groups were randomly assigned to treatment or control. Thioridazine solution was prepared in NaCl 0.9%. Perphenazine was solubilized in acidified 0.9% saline solution containing 0.005% acetic acid. Drugs and corresponding vehicles were administered in 250 μL intraperitoneally (i.p.). Injections were started when mice reached 70 days of age, before the obvious appearance of clinical symptoms. Animals were observed daily, weighed twice weekly and their motor function was assessed using a grid test and rotarod. Rotarod training was performed over three days with one 5 min trial per day. The rotarod (Ugo Basile 7650) was set to accelerate from 4 to 40 rpm over 300 s. Latency to fall was recorded in seconds (s) for each mouse. Motor tests were performed once a week in the afternoon. The survival endpoint was the loss of the righting reflex, *i.e.*, the inability of the animals to right themselves within 30 s after being laid on each side. Animals were euthanized with terminal anesthesia by Nembutal injection followed by intracardiac PBS perfusion prior to the collection of samples for protein and RNA extraction. For immunohistochemistry, paraformaldehyde (4% in PBS) was perfused prior to collection of samples.

2.12. Statistical analysis

Data were analysed using Graph-Pad Prism software 6.03. Student's *t*-test was used for cell culture experiments; non-parametric Mann-Whitney test was used for the experiments performed on animal samples; a one-way ANOVA for repeated measures with Bonferroni's Multiple Comparison Test post-hoc analysis was used for behaviour experiments; log-rank (Mantel-Cox) Test was used for lifespan comparison of treated *versus* vehicle SOD1^{G93A} mice.

3. Results

3.1. NOX2 and its subunits are strongly up-regulated in ALS spinal cord in mice and humans

The expression levels of all six mouse NOX isoforms and their subunits were measured by qPCR using RNA isolated from the spinal cord of wild-type (120 days) and SOD1^{G93A} mice at early (90 days) and terminal stage of disease (120 days) (Fig. 1A). DUOX1 and DUOX2 were below detection level (data not shown), but all other NOX isoforms were detected (Ct values are shown in Supplementary table 2). NOX3 was increased at similar levels at 90 and 120 days. NOX1, its subunits Noxo1 and Noxa1 or NOX4 did not show expression levels changes. Interestingly a subunit of DUOX1, DUOXA1 was detected in the spinal cord and its expression correlated with the disease progression. Expression of NOX2 and the subunits p22^{phox}, p47^{phox}, p67^{phox}, p40^{phox} and rac1 was significantly increased concomitantly with disease progression (Fig. 1A). Consistent with mRNA expression data, NOX2 protein was strongly increased in spinal cord of SOD1^{G93A} mice (120 days) (Fig. 1B). NOX mRNA expression was also measured in the spinal cord of two additional mouse models expressing ALS-causing genes, TDP-43 [23] and FUS/TLS [24] (Fig. 1C, D; see the materials and methods section for the description of these models). Similarly to SOD1^{G93A} mice, NOX2 expression was strongly increased in the spinal cord of TDP-43^{Q331K}, but not in TDP-43^{WT} mice at 12 months, as well as in symptomatic homozygous FUS/TLS^{WT} (40 days), but not in non-symptomatic heterozygous FUS/TLS^{WT} mice. However, while NOX4 expression was unaffected in the spinal cord of SOD1^{G93A} mice, NOX4 expression levels showed a trend to an increase in the spinal cord of TDP-43^{Q331K} (Fig. 1C) and significant increase in homozygous FUS/TLS^{WT} (Fig. 1D) mice at the late stages of disease. We were not able to detect NOX1 and NOX3 in the spinal cord of these mice. SOD1^{G93A} mice remain the best characterized model of ALS with visible clinical symptoms onset at about 90 days of age, progressive hind limb paralysis, massive motor neuron death, microgliosis and mortality at 120–140 days of age [22]. Therefore we used this animal model in the subsequent experiments. In human tissue, strong NOX2 immunostaining in the spinal cord from ALS patients was observed in cells with typical microglial morphology (Fig. 2). A trend towards increased levels of NOX2 in different regions of the spinal cord was observed in the patients as compared to non ALS controls.

3.2. Genetic deletion of NOX1 and 2 isoforms does not affect survival of SOD1^{G93A} mice

To assess the impact of NOX1 and NOX2 on the progression of neurodegeneration in ALS, we bred NOX1 and NOX2-deficient mice (normal life span) with SOD1^{G93A} mice and evaluated their survival. No significant change in survival was observed in neither mice deficient in NOX1 (Suppl. Fig. 2) nor NOX2 (Fig. 3A, B) for both genders when compared to wild-type ALS littermates. Interestingly, we observed that the B6 background increased survival of the SOD1^{G93A} male mice as previously shown by others [25,26]. Thus, the comparison between matched littermates is necessary to evaluate the effects of NOX deletion. NOX2 deficiency did not have an impact on the expression of neuronal (neurofilament light polypeptide, NEFL), microglial (Iba1, CD68) and astroglial markers (GFAP) neither in males nor in females (Fig. 3C). No obvious differences in morphology of activated microglia were detected in NOX2 deficient ALS mice (Suppl. Fig. 3).

Constitutive genetic ablation has limitations for validating the relevance of NOX targeting in ALS as i) NOX activity may be involved in neuronal development [2] and adaptive mechanisms might develop to compensate NOX-dependent signaling; ii) presence of NOX may be protective at early stages of ALS [27], iii) other NOX isoforms (*e.g.* NOX3, NOX4) might be involved in disease progression. Therefore, we also tested a pharmacological approach in order to inhibit all NOX, starting the treatment at early stage of disease (day 70).

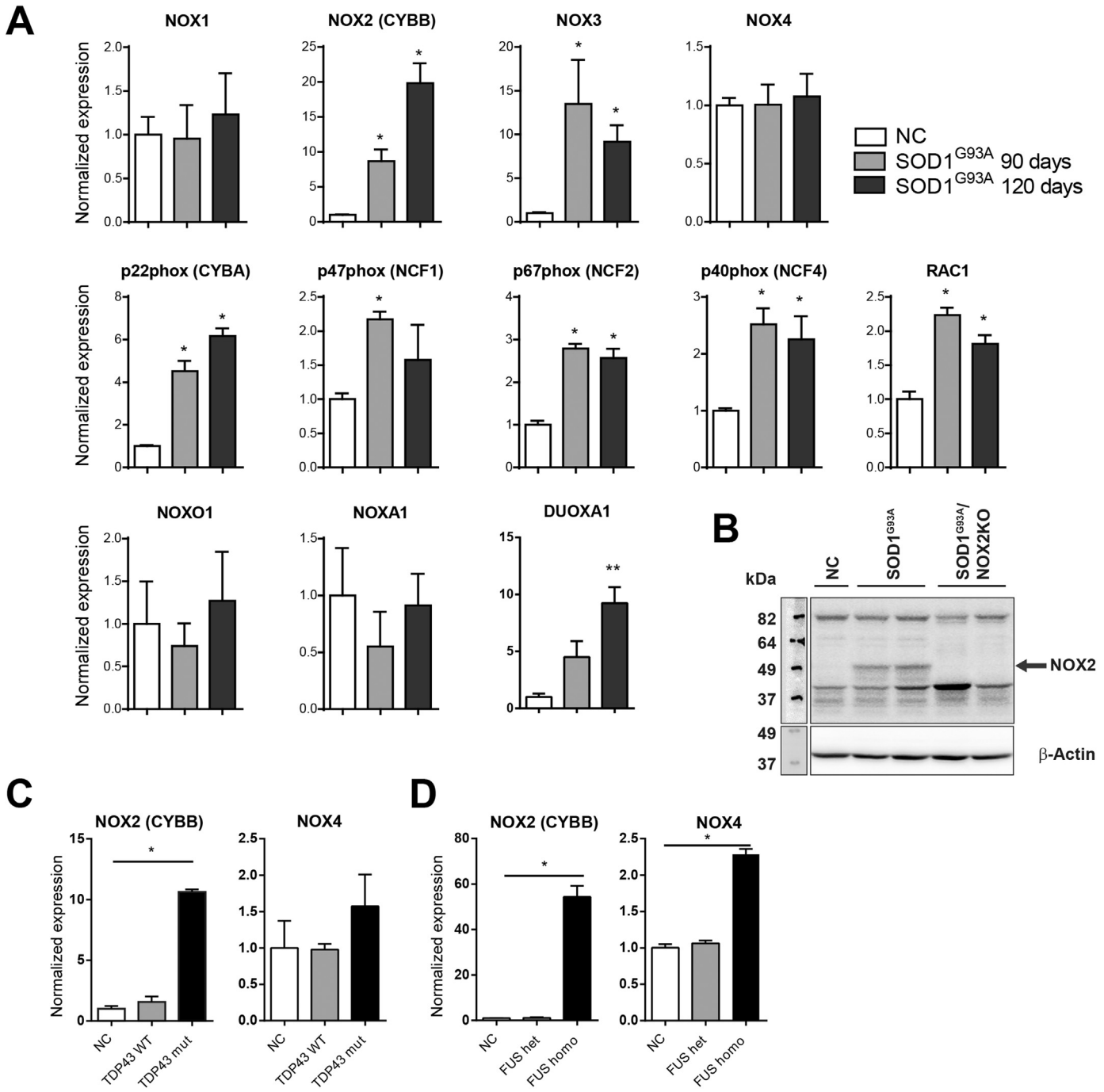

Fig. 1. NOX isoforms and subunits are upregulated in mouse models of ALS. (A) Quantitative real-time PCR was performed on mRNA from spinal cord of SOD1^{G93A} mice at different stages of disease (90 and 120 days, n=4 males) and for non-carrier littermates (120 days, n=4, males) for all NOX isoforms. NOX2 and NOX3 levels were strikingly increased and no change was observed for NOX1 and NOX4 levels while DUOX1 and DUOX2 levels were below detection level (data not shown). Consistent with NOX2 increase, the expression of subunits p22phox, p40phox, p47phox, p67phox and rac1 was increased already at early stage of disease, however the NOX1 and NOX3 subunits Noxo1 and Noxa1 were unchanged. DUOXA1 levels were increased with the progression of the disease. (B) Representative image of a western blot experiment showing detection of a 50 kDa NOX2-specific band in the spinal cord lysates of SOD1^{G93A} mice (final stage of disease), which is absent in NC mice (120 day) and SOD1^{G93A} mice bred with NOX2 deficient mice (final stage of disease). (C-D) Quantitative real-time PCR was performed also on mRNA from the spinal cord of two additional mouse models of ALS: (C) Increase in mRNA for NOX2 was found in the spinal cord of TDP-43^{Q331K}, but not in TDP^{WT} mice at 12 months (n=4, males and females), (D) Increased expression of NOX2 and NOX4 was observed in the spinal cord of symptomatic homozygous FUS/TLS^{WT}, but not in non-symptomatic heterozygous FUS/TLS^{WT} mice at 40 days (n=3, males and females). NOX1 and NOX3 levels were below detection threshold in these two models. For A, C, and D the values are expressed as a fold-change of NC mice, columns represent the mean ± SEM. Asterisks indicate a significant difference as determined by Mann-Whitney test (*$p < 0.05$).

3.3. *N-substituted phenothiazine compounds inhibit NOX-derived ROS generation by microglial cells*

The two N-substituted phenothiazine compounds, perphenazine and thioridazine (Fig. 4A), were chosen based on previous pharmacological characterization [12] for evaluation in an *in vitro* model of microglia activation. Pretreatment of cultured mouse microglial cells RA2 with 5 μg/mL LPS from *Escherichia coli* (Serotype R515 (Re)) lead to activated microglial morphology and increased expression of NOX2 (Fig. 4B) that was accompanied by an increase in PMA-induced production of ROS (Fig. 4C-D, dark grey *versus* light grey bars). To evaluate the effect of the two

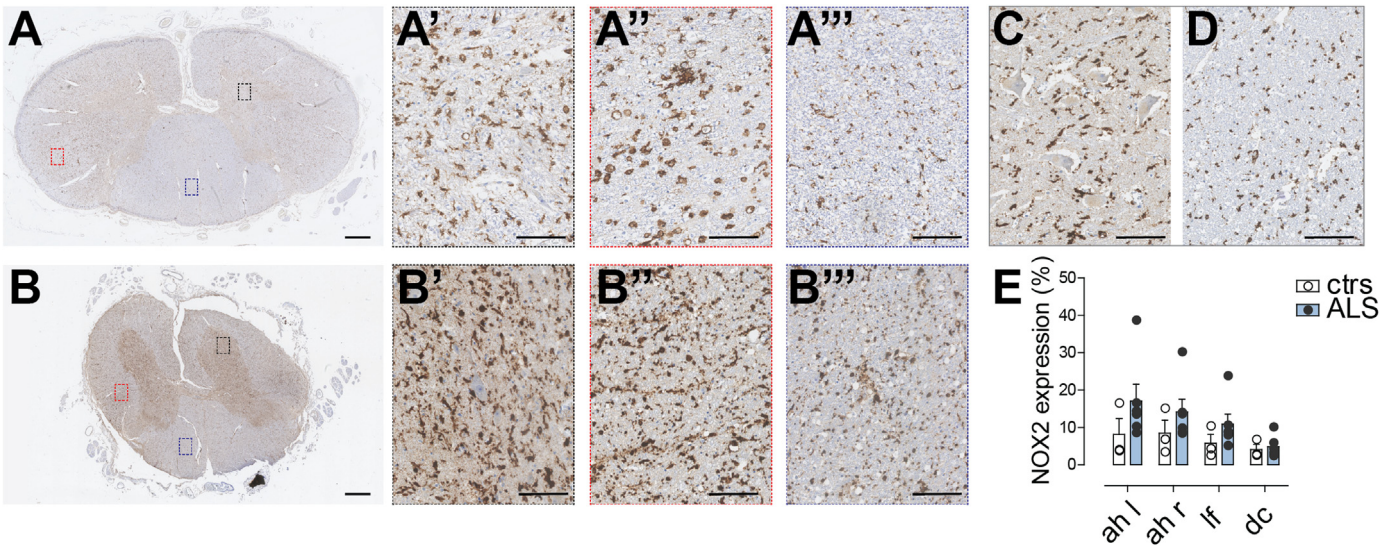

Fig. 2. NOX2 staining in ALS patients and controls. (A) and (B) NOX2-immunolabled cross sections of spinal cord from patients with amyotrophic lateral sclerosis (Scale bar: 1 mm). (A'-A''') and (B'-B''') show higher magnification (indicated by boxes in A and B) of anterior horn (A' and B'), lateral funiculus (A'' and B'') and dorsal columns (A''' and B'''). (C) and (D) depict anterior horn (C) and lateral funiculus (D) areas from a control case (Scale bar: 100 μm). (E) Bar graphs representing mean ± SEM for NOX2 protein expression, quantified as the percentage of the surface occupied by the NOX2 staining over the total measured area in selected regions: anterior horn left (ah l), anterior horn right (ah r), lateral funiculus (lf) and dorsal column (dc) of ALS and control (ctrs) patients (ALS, n=6; ctrs n=3). Each circle in (E) represents a measure for a separate case.

compounds on NOX2-derived ROS, we used two mechanistically different validated assays: the peroxidase-dependent Amplex Red fluorescent assay which measures H_2O_2, and the colorimetric WST-1 assay, which measures $O_2^{\bullet -}$ [16]. Both, perphenazine and thioridazine significantly inhibited generation of H_2O_2 and $O_2^{\bullet -}$ in this model (Fig. 4C, D). This indicated that the tested phenothiazines are able to diminish NOX2-derived ROS production by activated microglial cells, and they were further tested *in vivo*.

3.4. Pharmacokinetics of perphenazine and thioridazine in vivo

N-substituted phenothiazines are used in the clinic for CNS applications for over 50 years and their bioavailability in brain is well documented [28,29]. To ensure that concentrations of drug sufficient for NOX inhibition are obtained in the CNS, we administered perphenazine (3 mg/kg) or thioridazine (10 mg/kg) i.p. to wild type mice and measured the brain content of each drug after 0.5, 1, 2, 4 and 8 h. The brain concentration of perphenazine (Fig. 5A) and thioridazine (Fig. 5B) reached maximal level 2-4 h post injection, and these concentrations were above the respective IC_{50} values for NOX2 inhibition (3.9 ± 0.7 μM for perphenazine and 2.2 ± 0.2 μM for thioridazine in cellular assays [12]) at least for 8 h. The doses could not be increased to avoid the undesired sedative effect of these drugs.

3.5. Effect of thioridazine on spinal cord ROS generation in vivo

Increased expression of NOX2 leads to elevated oxidative modifications in ALS spinal cords [8]. Here, we assessed the specific reactive species generated in ALS spinal cords and NOX-inhibitory activity of thioridazine *in vivo*. For this, we used a LC/MS/MS detection system to differentiate the products of HE oxidation in the spinal cord $SOD1^{G93A}$ mice. In preliminary experiments we evaluated three different delivery routes for HE: i.p., i.v. and intraspinal injection. We noticed significant rapid oxidation of the probe in the plasma upon i.p. and i.v. injections (data not shown). In order to measure the specific oxidative activity occurring in the spinal cord parenchyma, we opted for direct intraspinal delivery of the probe for subsequent experiments. Thioridazine, 15 mg/kg, was administered to $SOD1^{G93A}$ mice i.p. 2 h prior to HE injection. The following HE oxidation products were detected and quantified in spinal cords: 2-hydroxyethidium (2-OH-E^+), the specific product of the reaction of HE with $O_2^{\bullet -}$ [30]; ethidium (E^+) non-specific product of HE oxidation; ethidium dimers (E^+dimer) [31] and 2-chlorethidium (2-Cl-E^+), a specific product formed from the reaction of HE with hypochlorous acid (HOCl) [21]. Consistent with an increase of oxidative stress in the ALS spinal cord, 2-OH-E^+ (Fig. 5C) [30] and E^+ dimer (Fig. 5E), but not E^+ (Fig. 5D) were increased in spinal cords of $SOD1^{G93A}$ mice during the clinical stage of the disease (110 days) as compared to NC littermates. We expressed these oxidation products relative to HE to account for possible differences in the concentration of the probe between animals. Indeed, standardization of results to HE improved the standard deviation. No difference in 2-chloroethidium (2-Cl-E^+) (Fig. 5F), an indicator of myeloperoxidase activity was observed in the spinal cord of $SOD1^{G93A}$ mice. Mice treated with thioridazine had significantly lower levels of HE-normalized 2-OH-E^+, the specific product of $O_2^{\bullet -}$ - induced HE oxidation and the primary product formed by NOX2- than vehicle-treated controls. This indicated that thioridazine indeed decreased ROS generation in the spinal cord of $SOD1^{G93A}$ mice, possibly through NOX2 inhibition (Fig. 5C).

3.6. Effect of perphenazine and thioridazine on disease progression and survival of $SOD1^{G93A}$ mice

To assess the efficacy of phenothiazine compounds *in vivo* in a mouse model of ALS perphenazine, thioridazine or their respective vehicles were administered i.p. daily to $SOD1^{G93A}$ mice starting at 70 days of age until terminal stage. We started the treatment at early stage of disease in order to target the switch of microglial activation state from protective to inflammatory which coincides with increased expression of NOX2 [27]. A summary of the experimental details is shown in Table 2.

Survival of $SOD1^{G93A}$ mice was evaluated following treatment with perphenazine (Fig. 6A) or thioridazine (Fig. 7A). The average survival values are shown in Table 2. None of the compounds significantly increased survival.

We assessed general progression of the disease by weight loss, motor performance (rotarod test), and muscle strength (time mice

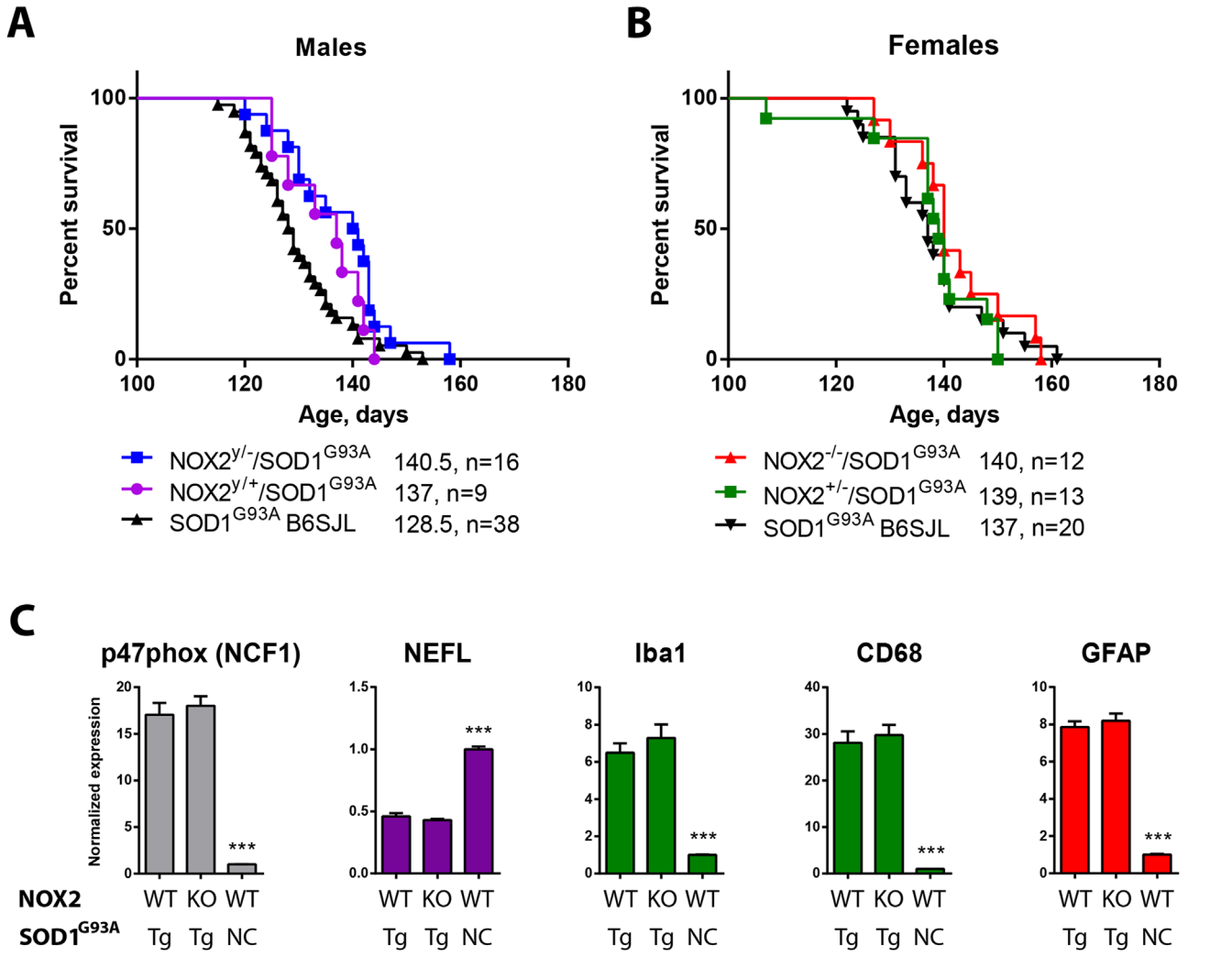

Fig. 3. Genetic ablation of NOX2 in SOD1^{G93A} mice does not improve survival or neurochemical markers. Survival of SOD1^{G93A} mice was compared to SOD1^{G93A}-NOX2 knockout mice (A) Double transgenic SOD1^{G93A} /NOX2 deficient hemizygous (NOX2$^{y/-}$, blue) males were compared to SOD1^{G93A} /WT littermates (NOX2$^{y/+}$, purple) and historical SOD1^{G93A} males in the hybrid B6SJL background (black), (B) Double transgenic SOD1^{G93A} /NOX2 deficient homozygous (NOX2$^{-/-}$, red) females were compared to SOD1^{G93A} /heterozygous littermates (NOX2$^{+/-}$, green) and historical SOD1^{G93A} females in the hybrid B6SJL background (black). Average survival and number of animals per group are indicated, log-rank (Mantel-Cox) test. (C) mRNA levels of the NOX2 subunit p47phox and neuronal (NEFL), microglial (Iba1, CD68) and astrocyte (GFAP) markers were assessed using qPCR in the spinal cord of SOD1^{G93A} mice crossed with NOX2 KO mice (n=6 males and n=5 females) and compared to NOX2 WT littermates (n=4 males and n=4 females) and non-carriers (n=4 males and n=4 females). Expression values were normalized to geometric mean of two house-keeping genes (GAPDH and HPRT) and expressed as a fold-change of SOD1^{G93A} non-carrier mice (NC). Values are presented as mean ± SEM. Mann-Whitney test, *$p < 0.05$, **$p < 0.01$, ***$p < 0.001$.

could stay upside down on a grid). Perphenazine treatment of SOD1^{G93A} mice resulted in significant improvement of body weight (Fig. 6B), but only a non-significant trend was seen in the rotarod and grid tests (Fig. 6C, D). Thioridazine treatment had no effect on weight loss of SOD1^{G93A} mice (Fig. 7B). Motor function was enhanced in the rotarod test immediately after the start of treatment (Fig. 7C); however, the deterioration of rotarod performance was comparable in thioridazine and vehicle treated mice. Muscle strength was not improved as shown by the grid test (Fig. 7D).

3.7. *Characterization of molecular markers*

We further evaluated molecular changes in the spinal cord of SOD1^{G93A} mice by qPCR and immunohistochemistry. Pharmacological inhibition of NOX2 did not produce a neuroprotective effect as shown by levels of the neurofilament light polypeptide (NEFL) mRNA (Fig. 8A, B) and quantification of motor neurons (Fig. 8C). Perphenazine treatment resulted in a trend to an increased expression of mRNA for micro- and astroglial markers, with a statistically significant increase of CD68 expression. However this effect was not confirmed by evaluation of immunostaining for microglial marker Iba1. Surprisingly, perphenazine increased the expression of NOX2 mRNA in the spinal cord of treated mice. On the other hand, thioridazine significantly decreased the expression levels of microglial markers Iba1 and CD68; moreover, a similar trend was observed in immunostaining for Iba1 in lumbar spinal cords of SOD1^{G93A} mice. Also, we observed a trend towards a decrease in expression of the astrocyte marker GFAP both at mRNA and protein levels in these animals. Interestingly, none of the evaluated markers showed a difference in NOX2-deficient *versus* control ALS mice (neither in males nor in females) (Fig. 3C), suggesting that the observed effects of phenothiazine compounds are pleiotropic.

4. Discussion

Curbing oxidative stress *via* phagocyte NADPH oxidase (aka gp91^{phox} or NOX2) inhibition has been proposed as a strategy for

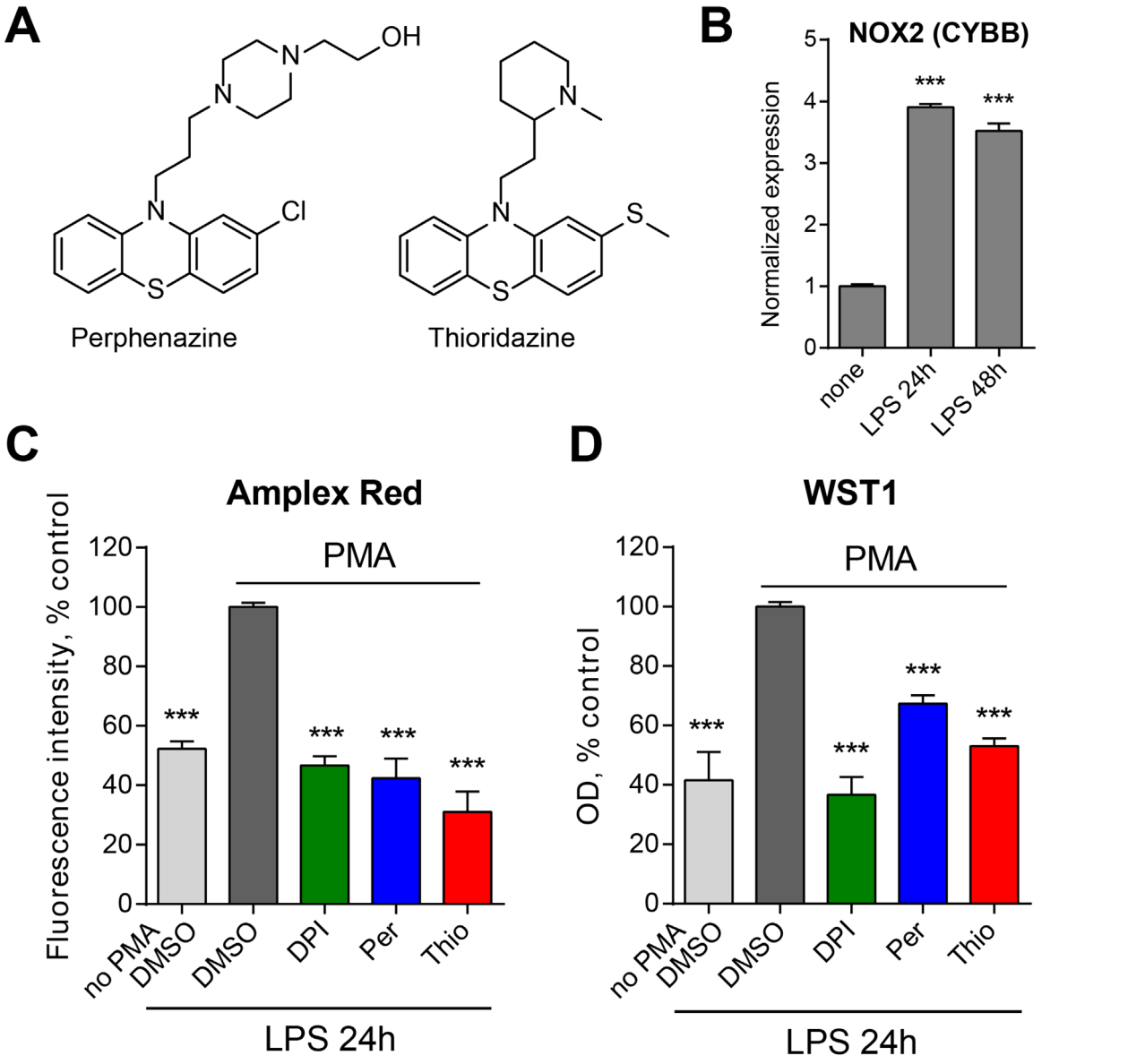

Fig. 4. Effect of perphenazine and thioridazine on ROS generation by microglial cells *in vitro*. (A) Chemical structures of the phenothiazines used in the study. (B) NOX2 mRNA expression is increased in RA2 cells upon treatment with LPS 5 μg/mL for 24 and 48 h (n=3). Columns show means ± SEM; asterisks indicate a significant difference from control (no LPS treatment) as determined by two-tailed unpaired Student's *t*-test (***$p < 0.001$). Tested compounds (10 μM) inhibit the production of (C) H_2O_2, Amplex Red assay and (D) superoxide radical anion, WST1 assay in RA2 cells pretreated with 5 μg/mL LPS for 48 h and stimulated with PMA 100 nM. The values obtained from 4 independent experiments were normalized to the control (RA2 cells pre-treated with LPS and treated with DMSO and PMA, 100%) and are presented as mean ± SEM. Student's *t*-test, *$p < 0.05$, **$p < 0.01$, ***$p < 0.001$. Per – perphenazine, Thio – thioridazine, OD – optical density.

the treatment of ALS [8,32]. This hypothesis has so far not been validated, as clinically relevant specific NOX2 inhibitors are not yet available. Apocynin, an antioxidant molecule with a complex mechanism of action [10,33] commonly advertised as a NOX inhibitor, has been administered to $SOD1^{G93A}$ mice; however, it failed to improve symptoms [34,35]. In an effort to identify small molecule NOX inhibitors, we have recently characterized thioridazine and other N-substituted phenothiazines as pan-NOX inhibitors [12]. Although phenothiazines have numerous modes of action in the CNS, they represent an interesting tool for target validation because their concentration in the CNS upon i.p. injection is compatible with NOX inhibition. In addition, perphenazine and thioridazine are already approved for human use allowing potential straightforward repositioning of these compounds into a clinical trial for ALS.

In a first set of experiments, we verified the induction of NOX2 expression in the CNS of ALS mice in three etiologically different disease models. This finding is compatible with involvement of NOX2 in a common pathomechanism for ALS and possibly other neurodegenerative disorders [7]. More detailed investigation in $SOD1^{G93A}$ mice showed NOX2 up-regulation at both transcriptional and protein levels and identified a related up-regulation of the subunits necessary for NOX2 activity. The levels of NOX2 are also increased in human ALS samples. We observed a typical microglial staining for NOX2 in human spinal cord, corroborating previous reports [7,8] and recent RNAseq data showing that NOX2 expression is restricted to microglia in the healthy mouse and human CNS ([36,37], see also http://web.stanford.edu/group/barres_lab/brain_rnaseq.html). NOX2 increase in the spinal cord of ALS mice and patients is most likely due to proliferation and activation of microglia although infiltration of mononuclear inflammatory cells may account at least in part for this increase. It is indeed difficult to distinguish the respective impact of macrophages and parenchymal microglia as they share the same specific

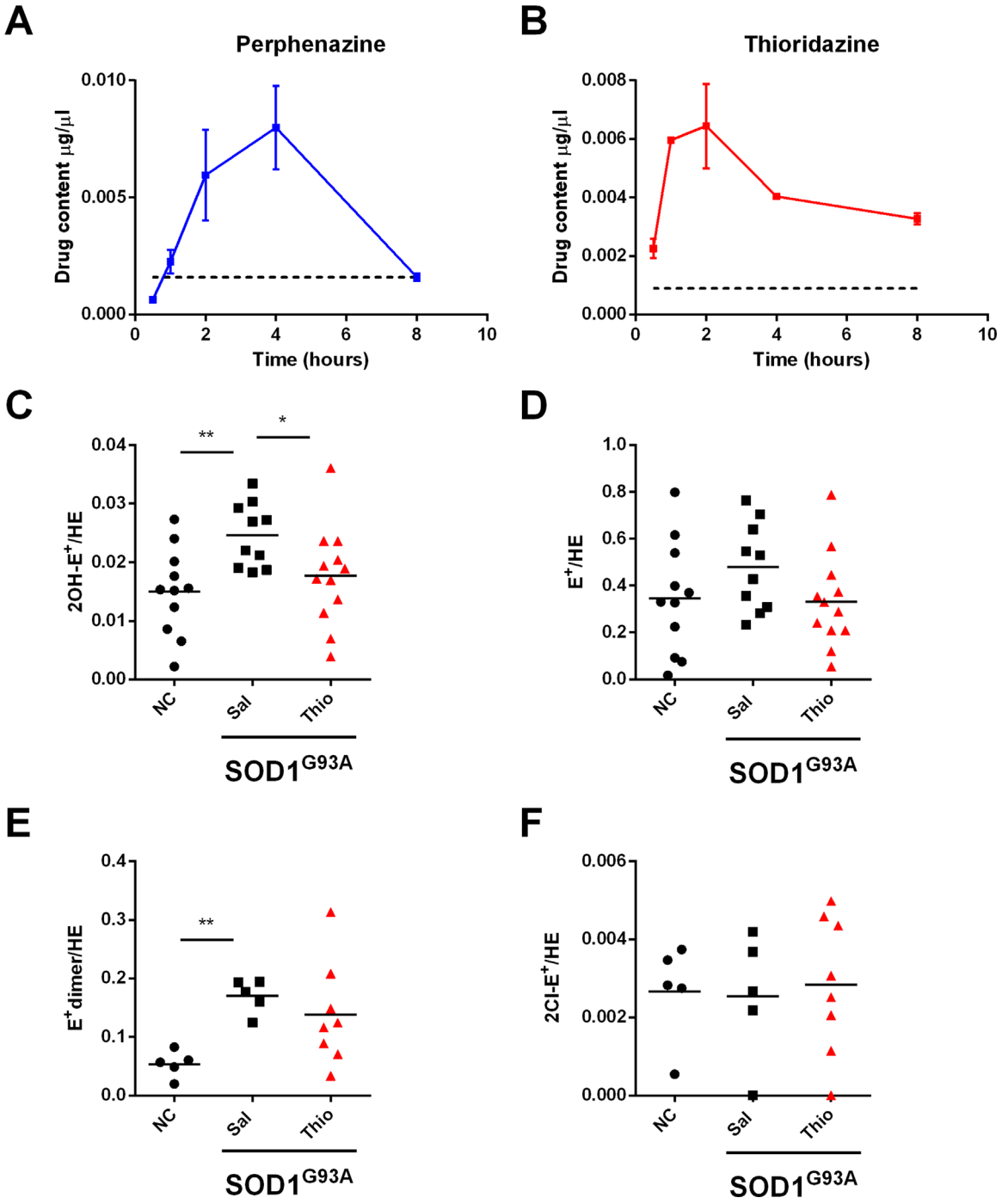

Fig. 5. *In vivo* pharmacology of perphenazine and thioridazine. Brain concentrations of compounds were determined upon i.p. injection of (A) perphenazine, 3 mg/kg and (B) thioridazine, 10 mg/kg. Dotted line shows IC_{50} value for NOX2 inhibition in Amplex red assay in PLB985 cells [12]. (C-F) LC/MS/MS quantification of HE oxidation products measured in the spinal cord tissue of $SOD1^{G93A}$ mice (females, 110 days) following administration of thioridazine or saline and non-carriers (NC). HE was administered intraspinally 30 min before collection of spinal cord. The following HE oxidation products were detected and quantified (C) 2-hydroxyethidium (2-OH-E^+), the specific product of the reaction of HE with $O_2^{\bullet-}$ [30]; (D) ethidium (E^+) and (E) ethidium dimers (E^+dimer) which are formed by unspecified oxidants [31] and (F) 2-chlorethidium (2-Cl-E^+), a specific product formed from the reaction of HE with hypochlorous acid (HOCl) [21]. The values are presented as ratio to total HE detected (individual values and mean). Mann-Whitney test, $^*p < 0.05$, $^{**}p < 0.01$. Thio – thioridazine.

Table 2
Treatment protocol.

Treatment	Gender	Dosage (mg/kg/d)	Mean survival (n) Vehicle	Drug	Log-rank test, p value
Perphenazine	Females	3	137 (30)	140 (31)	0.0838
Thioridazine	Females	10	132 (39)	134 (31)	0.3353

markers for both resting and active states, including NOX2. It is unlikely that the infiltration of T-lymphocytes accounts for this increase since the expression of NOX2 in T-cells is very low (if any) [38].

In contrast, based on the RNAseq data cited above, the presence of NOX4 in spinal cord homogenates might be due to its endothelial expression. The low level expression of NOX1 is likely due to vascular smooth muscle cells; however, the marked NOX3

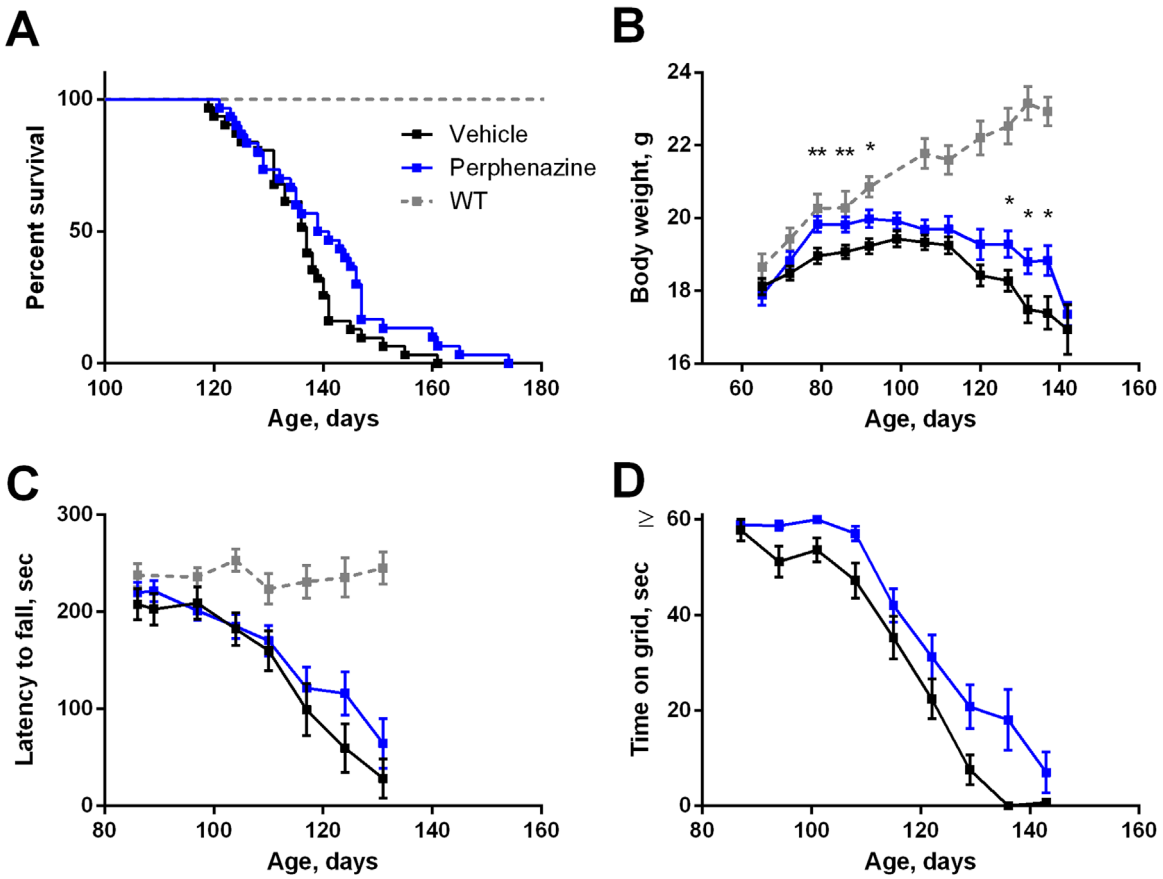

Fig. 6. Effect of perphenazine treatment on survival, weight and motor function of SOD1^{G93A} mice. Female SOD1^{G93A} mice were treated with perphenazine (3 mg/kg/day i.p). starting from day 70 until the end stage. (A) Survival: Log-rank (Mantel-Cox) Test shows no significant differences in survival of mice treated with perphenazine (n=31) as compared to vehicle treated mice (n=30). (B) Body weight: slight improvement in body weight loss was detected in perphenazine treated mice as compared to vehicle treated mice (n=42 per group up to 110 days, n=30 per group until the terminal stage), *t*-test performed for each time point to compare treatment *versus* vehicle, $^{*}p < 0.05$; $^{**}p < 0.005$. (C) Rotarod: no improvement in motor function was detected (n=24 vehicle; n=25 perphenazine). (D) Grid test: no improvement of motor function was observed in this test, n=31 per group. Traces from historical control NC littermates are shown in (A - C) as grey dotted line (n=12).

upregulation in the SOD1^{G93A} model is puzzling and was not anticipated since NOX3 expression is almost completely restricted to the inner ear and to embryonic tissue. Unfortunately, the lack of validated mouse NOX3 antibodies is a limitation to identify the specific cellular localization of NOX3 in the spinal cord of ALS mice. Another interesting observation is that DUOXA1 is expressed in the spinal cord tissue and upregulated with the course of the disease. DUOXA1 is known as a subunit necessary for the activity of DUOX1. However DUOX1 was below detection levels in the analyzed tissues. This suggests a possible role for DUOXA1 in the CNS which is independent of DUOX1.

Importantly, the increase in the expression of NOX enzymes was accompanied by an increase of ROS in the spinal cord *in vivo*. We used LC/MS/MS analysis of HE and its oxidation products as, unlike the standard fluorescence detection of HE oxidation, it allows for the detection and quantification of specific products of HE oxidation, including those with $O_2^{\bullet -}$ and hypochlorous acid, the latter usually produced by MPO in activated neutrophils. This method indicated that general oxidation is increased in the spinal cord of SOD1^{G93A} mice, but also that the increased levels of $O_2^{\bullet -}$, the specific primary product of NOX, were decreased in thioridazine-treated animals, compatible with the notion that NOX is inhibited *in vivo*. Conversely, the levels of chlorinated HE, the product of MPO activity, were unchanged. The absence of MPO activity likely reflects the absence of neutrophil infiltration in the spinal cord of ALS mice. Interestingly, the increase in ROS measured in spinal cord (1.5-fold) appears substantially lower than the induction of NOX2 mRNA (> 20-fold) in ALS spinal cord. This may suggest that although NOX2 is present, it may not be fully activated. The expression of regulatory subunits (p47^{phox}, p67^{phox} and p40^{phox}) shows 2–5 fold increase. This might limit NOX2-derived superoxide generation since the active complex requires equimolar assembly of all subunits. In addition NOX2 requires activation for the generation of ROS. This is illustrated by ROS measurements in microglial cells: increased NOX2 expression upon LPS pretreatment is not sufficient to generate ROS and requires additional stimulation with PMA, a PKC activator. In addition to NOX, other sources of ROS, including mitochondria, xanthine oxidase, cytochrome P450 or iNOS, may be relevant sources of oxidative stress in ALS and other neuroinflammatory conditions [39–41]. It is possible that thioridazine interferes with one or several of these systems [42,43].

Despite strong up-regulation of the NOX2 complex in SOD1^{G93A} mice, associated with increased $O_2^{\bullet -}$ *in vivo*, which can be mitigated by thioridazine treatment, we found no improvement in survival following pharmacological intervention with thioridazine or perphenazine. A possible explanation for the lack of impact on survival of the N-substituted phenothiazine treatment is their insufficient CNS exposure. Although the concentrations of perphenazine and thioridazine in the CNS were above or higher than the IC_{50} for NOX2 inhibition for at least 8 h, we cannot exclude that CNS exposure obtained upon a single injection of the drug was not sufficient in a 24 h period. We selected a single daily dose in order to avoid long period of drowsiness in mice induced by high doses of phenothiazines. Another possible explanation is that NOX inhibition alone is insufficient to slow down disease progression and

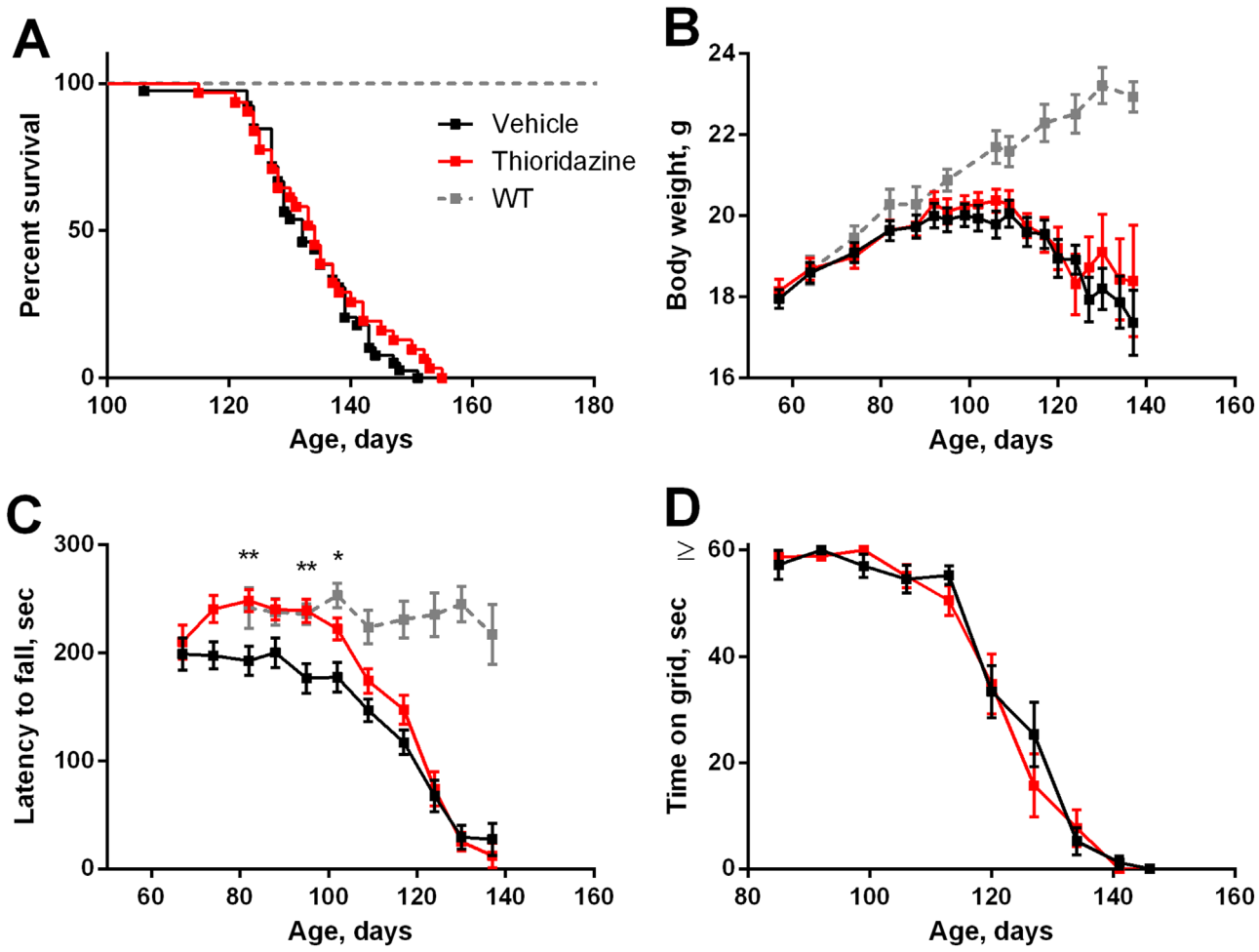

Fig. 7. Effect of thioridazine treatment on survival, weight and motor function of SOD1^{G93A} mice. Female SOD1^{G93A} mice were treated with thioridazine (10 mg/kg/day i.p). starting from day 70 until the end stage. (A) Survival: Log-rank (Mantel-Cox) Test shows no significant differences in survival of mice treated with thioridazine (n=31) as compared to vehicle treated mice (n=39). (B) Body weight: no improvement was detected in thioridazine treated mice (n=30) as compared to vehicle treated mice (n=30). (C) Rotarod: improvement of motor function was detected at the early symptomatic stage of the disease (Two way ANOVA followed by Bonferroni multiple comparisons test, n=30 per group); no differences between groups were observed at the later stages of disease. (D) Grid test: no improvement of motor function was observed in this test, n=30 per group. Traces from historical control NC littermates are shown in (A - C) as grey dotted line (n=12).

to improve survival as the breeding of SOD1^{G93A} mice with NOX1 and NOX2-deficient mice did not impact the survival or motor neuron loss. Our results are in disagreement with previous studies, which reported increased survival of 13 days [8] and 97 days [32] of ALS mice cross-bred with NOX2-deficient mice and 33 days for NOX1 genetic ablation [32]. The discrepancy with the first report (13 days) is most likely due to genetic background effect. SOD1^{G93A} mice used in this study are in the hybrid B6/SJL background while NOX2-deficient mice are in the B6 background. The survival of mice with SOD1^{G93A} mutation is increased when the transgene is carried in a pure B6 background [25]. We similarly observed an increased survival of 12 days in males in the mixed background compared to the hybrid background for both breeding with NOX2 and NOX1-deficient mice. The massive survival effect of NOX2 (and to a less extent NOX1) deletion reported by others [32] could not be reproduced. In our study, we followed specific standard operating procedures for pharmacological treatments [44] and used non-carrier littermates as control for evaluation of survival. Inducible genetic ablation of NOX2 specifically in microglia would provide a further insight into its contribution to the progression of ALS.

Although chronic administration of perphenazine or thioridazine failed to improve the survival of ALS mice, both molecules modified specific molecular markers and clinical symptoms in this model. Undeniably, in addition to NOX inhibitory activity, perphenazine and thioridazine have multiple actions in the CNS, such as D2 dopamine receptor antagonism, among others (reviewed in [45,46]). Strikingly, despite high structural similarities, the two N-substituted phenothiazines tested in this study had opposite effects on glial markers. Perphenazine treatment showed an increase of the expression of NOX2 and CD68 and a trend to an increase of GFAP and Iba1, while thioridazine treatment had the opposite effect. The reason for this difference is unclear, however we cannot exclude that the less favorable pharmacokinetics profile of perphenazine is involved. Besides, different aspects of disease progression were affected by the two treatments. Perphenazine slowed down the weight loss of SOD1^{G93A} mice, which could be explained by the known weigh gain promoting effect of antipsychotics [47]. Thioridazine treatment resulted in an immediate enhancement of rotarod performance to the level of controls during early disease stages (day 70–day 100). This is a potentially interesting finding; however it is not clear whether this effect is due to NOX inhibition.

5. Conclusion

In this study, we demonstrate that the expression of NOX2 isoform of the NADPH oxidase family is strongly increased in the

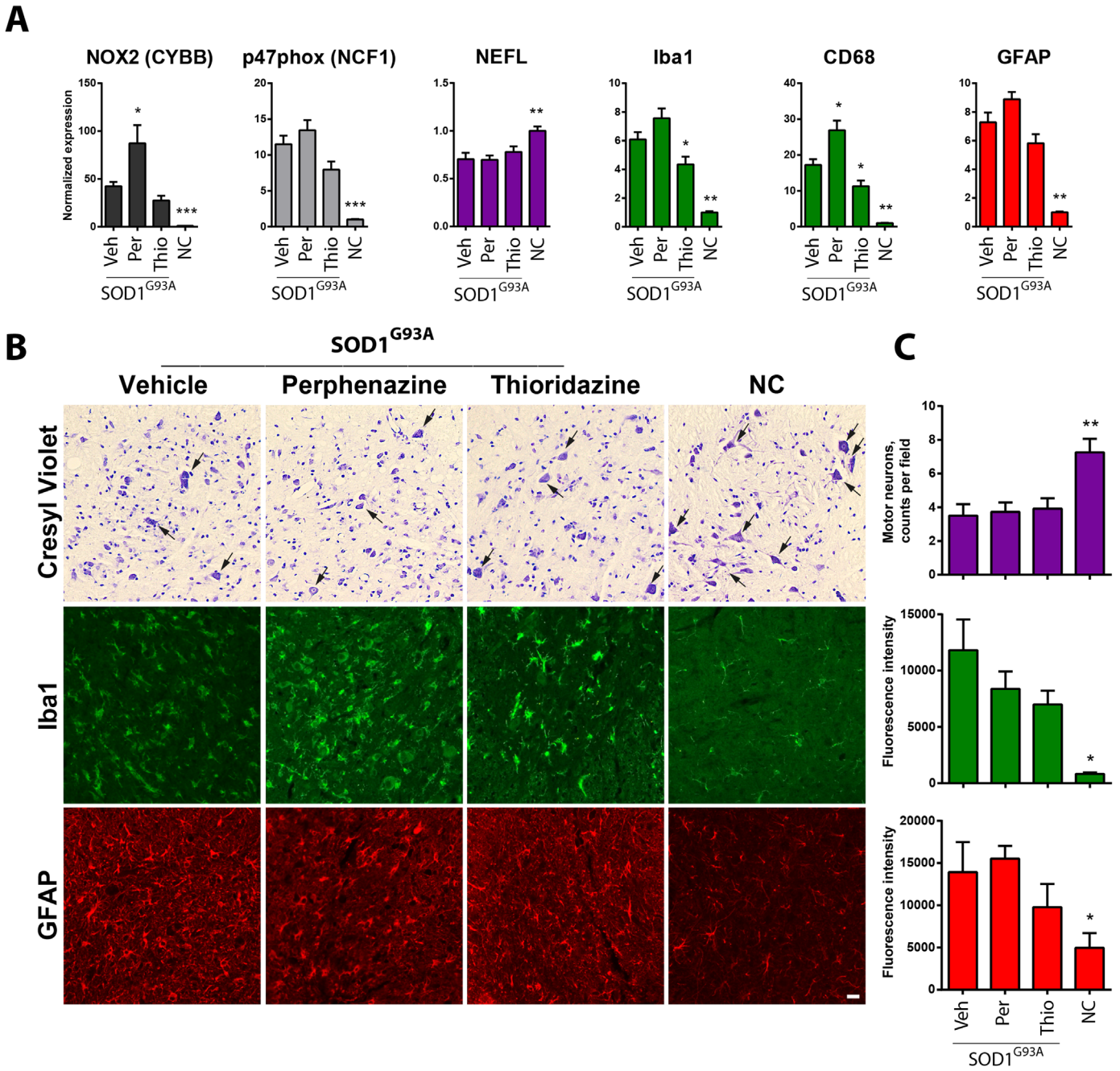

Fig. 8. Analysis of neuronal and glial markers expression in spinal cord of SOD1^{G93A} mice treated with perphenazine or thioridazine. (A) mRNA levels of NOX2 and its subunit p47phox and neuronal (NEFL), microglial (Iba1, CD68) and astrocyte (GFAP) markers were assessed using qPCR in the spinal cord of (A) SOD1^{G93A} mice aged 110–115 days treated with perphenazine (n=7) or thioridazine (n=6) and compared to vehicle-treated mice (n=7) and SOD1^{G93A} non-carrier mice (NC) (n=6), Expression values were normalized to geometric mean of two house-keeping genes (GAPDH and HPRT) and expressed as a fold-change of SOD1^{G93A} non-carrier mice (NC). Values are presented as mean ± SEM. Mann-Whitney test, $^{*}p < 0.05$, $^{**}p < 0.01$, $^{***}p < 0.001$. (B) Immunohistochemical analysis of neuronal (Cresyl violet, arrows indicate surviving motor neurons), microglial (Iba1) and astrocyte (GFAP) markers in lumbar spinal cord of SOD1^{G93A} mice aged 110–115 days. n=3 per group. Scale bar −25 μM. Images were taken in the area corresponding to ventral horn. (C) Quantification of immunostaining in B.

spinal cord of ALS models. NOX2 expression is microglia specific and correlates with the level of microgliosis and severity of disease. As opposed to former studies, constitutive genetic deletion of NOX1 or NOX2 did not improve survival of ALS mice. Using a novel LC/MS/MS based method we were able to detect specific increase of intraspinal superoxide in ALS mice, which could be mitigated by thioridazine, a broad spectrum NOX inhibitor. Thioridazine showed favorable CNS pharmacokinetics and moderate enhancement of motor function without an impact on the later disease stages and mortality. While thioridazine is an imperfect tool to study the involvement of NOX in ALS, novel effort for identification of NOX2 inhibitors [11] and the recently discovered BBB permeable specific NOX2 inhibitor GSK2795039 [10] may represent favorable approaches for further validation of the therapeutic potential of NOX inhibition for the treatment of ALS and other neurodegenerative diseases.

Competing interests

The author(s) declare that they have no competing interests.

Authors' contributions

TS and VJ conceived the study, designed and performed experiments, analyzed the data and wrote the manuscript. ZN performed qPCRs, injected animals and collected material. OB and OP performed genotyping, injections and material collection. AF performed immunohistochemistry and cell counts on mouse spinal cords. SS, MTG and ER performed NOX2 immunohistochemistry on human spinal cord tissue. SCL and DWC generated the samples for TDP43 and FUS ALS mouse models used in the studies. GM performed LC-MS/MS analysis of hydroethidine oxidation products in mouse spinal cords. KHK, DWC, AA and RS conceived the study and edited the manuscript. All authors read and approved the final manuscript.

Acknowledgments

We are thankful to Stéphanie Julien for help injecting SOD1^{G93A} mice over the weekends; to Christelle Barraclough and Didier Chollet for assistance with qPCRs; to Marie Pertin for the training for intraspinal injections. This study was granted by the European Community's Framework Programme (FP7/2007–2013) under Grant 278611 (Neurinox) and was partially supported by a National Health and Medical Research Council of Australia (NHMRC) grant (10307879) to RS. Vincent Jaquet and Olivier Basset were supported by a grant from the Swiss innovation promotion agency CTI (Grant no. KTI-NR.9958.1PFLS-LS). RS was supported by a Senior Principal Research Fellowship from the NHMRC.

Appendix A. Supporting information

Supplementary data associated with this article can be found in the online version at http://dx.doi.org/10.1016/j.freeradbiomed.2016.05.016.

References

[1] D. Brites, A.R. Vaz, Microglia centered pathogenesis in ALS: insights in cell interconnectivity, Front. Cell. Neurosci. 8 (2014) 117, http://dx.doi.org/10.3389/fncel.2014.00117.
[2] Z. Nayernia, V. Jaquet, K.H. Krause, New insights on NOX enzymes in the central nervous system, Antioxid. Redox Signal. 20 (17) (2014) 2815–2837, http://dx.doi.org/10.1089/ars.2013.5703.
[3] T.L. Leto, S. Morand, D. Hurt, T. Ueyama, Targeting and regulation of reactive oxygen species generation by Nox family NADPH oxidases, Antioxid. Redox Signal. 11 (10) (2009) 2607–2619, http://dx.doi.org/10.1089/ARS.2009.2637.
[4] K. Bedard, K.H. Krause, The NOX family of ROS-generating NADPH oxidases: physiology and pathophysiology, Physiol. Rev. 87 (1) (2007) 245–313, http://dx.doi.org/10.1152/physrev.00044.2005.
[5] D.H. Choi, A.C. Cristovao, S. Guhathakurta, J. Lee, T.H. Joh, M.F. Beal, et al., NADPH oxidase 1-mediated oxidative stress leads to dopamine neuron death in Parkinson's disease, Antioxid. Redox Signal. (2012), http://dx.doi.org/10.1089/ars.2011.3960.
[6] C. Kleinschnitz, H. Grund, K. Wingler, M.E. Armitage, E. Jones, M. Mittal, et al., Post-stroke inhibition of induced NADPH oxidase type 4 prevents oxidative stress and neurodegeneration, PLoS Biol. 8 (9) (2010), http://dx.doi.org/10.1371/journal.pbio.1000479.
[7] S. Sorce, M. Nuvolone, A. Keller, J. Falsig, A. Varol, P. Schwarz, et al., The role of the NADPH oxidase NOX2 in prion pathogenesis, PLoS Pathog. 10 (12) (2014) e1004531, http://dx.doi.org/10.1371/journal.ppat.1004531.
[8] D.C. Wu, D.B. Re, M. Nagai, H. Ischiropoulos, S. Przedborski, The inflammatory NADPH oxidase enzyme modulates motor neuron degeneration in amyotrophic lateral sclerosis mice, Proc. Natl. Acad. Sci. USA 103 (32) (2006) 12132–12137, http://dx.doi.org/10.1073/pnas.0603670103.
[9] G. Marrali, F. Casale, P. Salamone, G. Fuda, C. Caorsi, A. Amoroso, et al., NADPH oxidase (NOX2) activity is a modifier of survival in ALS, J. Neurol. 261 (11) (2014) 2178–2183, http://dx.doi.org/10.1007/s00415-014-7470-0.
[10] K. Hirano, W.S. Chen, A.L. Chueng, A.A. Dunne, T. Seredenina, A. Filippova, et al., Discovery of GSK2795039, a novel small molecule NADPH oxidase 2 inhibitor, Antioxid. Redox Signal. (2015), http://dx.doi.org/10.1089/ars.2014.6202.
[11] J. Zielonka, M. Zielonka, L. VerPlank, G. Cheng, M. Hardy, O. Ouari, et al., Mitigation of NADPH oxidase 2 activity as a strategy to inhibit peroxynitrite formation, J. Biol. Chem. (2016), http://dx.doi.org/10.1074/jbc.M115.702787.
[12] T. Seredenina, G. Chiriano, A. Filippova, Z. Nayernia, Z. Mahiout, L. Fioraso-Cartier, et al., A subset of N-substituted phenothiazines inhibits NADPH oxidases, Free Radic. Biol. Med. (2015), http://dx.doi.org/10.1016/j.freeradbiomed.2015.05.023.
[13] M.J. Ohlow, B. Moosmann, Phenothiazine: the seven lives of pharmacology's first lead structure, Drug Discov. Today 16 (3–4) (2011) 119–131, http://dx.doi.org/10.1016/j.drudis.2011.01.001.
[14] T. Kanzawa, M. Sawada, K. Kato, K. Yamamoto, H. Mori, R. Tanaka, Differentiated regulation of allo-antigen presentation by different types of murine microglial cell lines, J. Neurosci. Res. 62 (3) (2000) 383–388.
[15] V. Jaquet, J. Marcoux, E. Forest, K.G. Leidal, S. McCormick, Y. Westermaier, et al., NADPH oxidase (NOX) isoforms are inhibited by celastrol with a dual mode of action, Br. J. Pharmacol. 164 (2b) (2011) 507–520, http://dx.doi.org/10.1111/j.1476-5381.2011.01439.x.
[16] A.S. Tan, M.V. Berridge, Superoxide produced by activated neutrophils efficiently reduces the tetrazolium salt, WST-1 to produce a soluble formazan: a simple colorimetric assay for measuring respiratory burst activation and for screening anti-inflammatory agents, J. Immunol. Methods 238 (1-2) (2000) 59–68.
[17] J. Zielonka, M. Zielonka, A. Sikora, J. Adamus, J. Joseph, M. Hardy, et al., Global profiling of reactive oxygen and nitrogen species in biological systems: high-throughput real-time analyses, J. Biol. Chem. 287 (5) (2012) 2984–2995, http://dx.doi.org/10.1074/jbc.M111.309062.
[18] D. Debski, R. Smulik, J. Zielonka, B. Michalowski, M. Jakubowska, K. Debowska, et al., Mechanism of oxidative conversion of Amplex(R) Red to resorufin: pulse radiolysis and enzymatic studies, Free Radic. Biol. Med. 95 (2016) 323–332, http://dx.doi.org/10.1016/j.freeradbiomed.2016.03.027.
[19] J. Vandesompele, , K. De Preter, F. Pattyn, B. Poppe, N. Van Roy, A. De Paepe, Accurate normalization of real-time quantitative RT-PCR data by geometric averaging of multiple internal control genes, Genome Biol. 3 (7) (2002), RESEARCH0034.
[20] H.W. Bothe, W. Bodsch, K.A. Hossmann, Relationship between specific gravity, water content, and serum protein extravasation in various types of vasogenic brain edema, Acta Neuropathol. 64 (1) (1984) 37–42.
[21] G.J. Maghzal, K.M. Cergol, S.R. Shengule, C. Suarna, D. Newington, A.J. Kettle, et al., Assessment of myeloperoxidase activity by the conversion of hydroethidine to 2-chloroethidium, J. Biol. Chem. 289 (9) (2014) 5580–5595, http://dx.doi.org/10.1074/jbc.M113.539486.
[22] M.E. Gurney, H. Pu, A.Y. Chiu, M.C. Dal Canto, C.Y. Polchow, D.D. Alexander, et al., Motor neuron degeneration in mice that express a human Cu, Zn superoxide dismutase mutation, Science 264 (5166) (1994) 1772-5.
[23] E.S. Arnold, S.C. Ling, S.C. Huelga, C. Lagier-Tourenne, M. Polymenidou, D. Ditsworth, et al., ALS-linked TDP-43 mutations produce aberrant RNA splicing and adult-onset motor neuron disease without aggregation or loss of nuclear TDP-43, Proc. Natl. Acad. Sci. USA 110 (8) (2013) E736–45, http://dx.doi.org/10.1073/pnas.1222809110.
[24] S. Sun, S.C. Ling, J. Qiu, C.P. Albuquerque, Y. Zhou, S. Tokunaga, et al., ALS-causative mutations in FUS/TLS confer gain and loss of function by altered association with SMN and U1-snRNP, Nat. Commun. 6 (2015) 6171, http://dx.doi.org/10.1038/ncomms7171.
[25] T.D. Heiman-Patterson, J.S. Deitch, E.P. Blankenhorn, K.L. Erwin, M.J. Perreault, B.K. Alexander, et al., Background and gender effects on survival in the TgN (SOD1-G93A)1Gur mouse model of ALS, J. Neurol. Sci. 236 (1–2) (2005) 1–7, http://dx.doi.org/10.1016/j.jns.2005.02.006.
[26] A.C. Ludolph, C. Bendotti, E. Blaugrund, B. Hengerer, J.P. Loffler, J. Martin, et al., Guidelines for the preclinical in vivo evaluation of pharmacological active drugs for ALS/MND: report on the 142nd ENMC international workshop, Amyotroph. Lateral Scler. 8 (4) (2007) 217–223, http://dx.doi.org/10.1080/17482960701292837.
[27] B. Liao, W. Zhao, D.R. Beers, J.S. Henkel, S.H. Appel, Transformation from a neuroprotective to a neurotoxic microglial phenotype in a mouse model of ALS, Exp. Neurol. 237 (1) (2012) 147–152, http://dx.doi.org/10.1016/j.expneurol.2012.06.011.
[28] W.A. Daniel, M. Syrek, A. Haduch, J. Wojcikowski, Pharmacokinetics and metabolism of thioridazine during co-administration of tricyclic antidepressants, Br. J. Pharmacol. 131 (2) (2000) 287–295, http://dx.doi.org/10.1038/sj.bjp.0703540.
[29] W.A. Daniel, Mechanisms of cellular distribution of psychotropic drugs. Significance for drug action and interactions, Progr. Neuro-psychopharmacol. Biol. Psychiatry 27 (1) (2003) 65–73.
[30] J. Zielonka, J. Vasquez-Vivar, B. Kalyanaraman, Detection of 2-hydroxyethidium in cellular systems: a unique marker product of superoxide and hydroethidine, Nat. Protoc. 3 (1) (2008) 8–21, http://dx.doi.org/10.1038/nprot.2007.473.
[31] J. Zielonka, B. Kalyanaraman, Hydroethidine- and MitoSOX-derived red fluorescence is not a reliable indicator of intracellular superoxide formation: another inconvenient truth, Free Radic. Biol. Med. 48 (8) (2010) 983–1001, http://dx.doi.org/10.1016/j.freeradbiomed.2010.01.028.
[32] J.J. Marden, M.M. Harraz, A.J. Williams, K. Nelson, M. Luo, H. Paulson, et al., Redox modifier genes in amyotrophic lateral sclerosis in mice, J. Clin. Investig. 117 (10) (2007) 2913–2919, http://dx.doi.org/10.1172/JCI31265.
[33] S. Heumuller, S. Wind, E. Barbosa-Sicard, H.H. Schmidt, R. Busse, K. Schroder,

et al., Apocynin is not an inhibitor of vascular NADPH oxidases but an antioxidant, Hypertension 51 (2) (2008) 211–217, http://dx.doi.org/10.1161/HYPERTENSIONAHA.107.100214.
[34] K.A. Trumbull, D. McAllister, M.M. Gandelman, W.Y. Fung, T. Lew, L. Brennan, et al., Diapocynin and apocynin administration fails to significantly extend survival in G93A SOD1 ALS mice, Neurobiol. Dis. 45 (1) (2012) 137–144, http://dx.doi.org/10.1016/j.nbd.2011.07.015.
[35] J.M. Lincecum, F.G. Vieira, M.Z. Wang, K. Thompson, G.S. De Zutter, J. Kidd, et al., From transcriptome analysis to therapeutic anti-CD40L treatment in the SOD1 model of amyotrophic lateral sclerosis, Nat. Genet. 42 (5) (2010) 392–399, http://dx.doi.org/10.1038/ng.557.
[36] Y. Zhang, K. Chen, S.A. Sloan, M.L. Bennett, A.R. Scholze, S. O'Keeffe, et al., An RNA-sequencing transcriptome and splicing database of glia, neurons, and vascular cells of the cerebral cortex, J. Neurosci. 34 (36) (2014) 11929–11947, http://dx.doi.org/10.1523/JNEUROSCI.1860-14.2014.
[37] M.L. Bennett, F.C. Bennett, S.A. Liddelow, B. Ajami, J.L. Zamanian, N.B. Fernhoff, et al., New tools for studying microglia in the mouse and human CNS, Proc. Natl. Acad. Sci. USA (2016), http://dx.doi.org/10.1073/pnas.1525528113.
[38] K.A. Gelderman, M. Hultqvist, A. Pizzolla, M. Zhao, K.S. Nandakumar, R. Mattsson, et al., Macrophages suppress T cell responses and arthritis development in mice by producing reactive oxygen species, J. Clin. Investig. 117 (10) (2007) 3020–3028, http://dx.doi.org/10.1172/JCI31935.
[39] J. Lee, H. Ryu, N.W. Kowall, Differential regulation of neuronal and inducible nitric oxide synthase (NOS) in the spinal cord of mutant SOD1 (G93A) ALS mice, Biochem. Biophys. Res. Commun. 387 (1) (2009) 202–206, http://dx.doi.org/10.1016/j.bbrc.2009.07.007.
[40] A. Panov, N. Kubalik, N. Zinchenko, R. Hemendinger, S. Dikalov, H. L. Bonkovsky, Respiration and ROS production in brain and spinal cord mitochondria of transgenic rats with mutant G93a Cu/Zn-superoxide dismutase gene, Neurobiol. Dis. 44 (1) (2011) 53–62, http://dx.doi.org/10.1016/j.nbd.2011.06.003.
[41] F. Rezende, O. Loewe, V. Helfinger, K.K. Prior, M. Walter, S. Zukunft, et al., Unchanged NADPH oxidase activity in Nox1-Nox2-Nox4 triple knockout mice - What do NADPH-stimulated chemiluminescence assays really detect? Antioxid. Redox Signal. (2015), http://dx.doi.org/10.1089/ars.2015.6314.
[42] T. Rodrigues, A.C. Santos, A.A. Pigoso, F.E. Mingatto, S.A. Uyemura, C. Curti, Thioridazine interacts with the membrane of mitochondria acquiring antioxidant activity toward apoptosis–potentially implicated mechanisms, Br. J. Pharmacol. 136 (1) (2002) 136–142, http://dx.doi.org/10.1038/sj.bjp.0704672.
[43] C. Van den Branden, F. Roels, Thioridazine: a selective inhibitor of peroxisomal beta-oxidation in vivo, FEBS Lett. 187 (2) (1985) 331–333.
[44] A.C. Ludolph, C. Bendotti, E. Blaugrund, A. Chio, L. Greensmith, J.P. Loeffler, et al., Guidelines for preclinical animal research in ALS/MND: a consensus meeting, Amyotroph. Later. Scler. 11 (1–2) (2010) 38–45, http://dx.doi.org/10.3109/17482960903545334.
[45] G. Sudeshna, K. Parimal, Multiple non-psychiatric effects of phenothiazines: a review, Eur. J. Pharmacol. 648 (1–3) (2010) 6–14, http://dx.doi.org/10.1016/j.ejphar.2010.08.045.
[46] A. Jaszczyszyn, K. Gasiorowski, P. Swiatek, W. Malinka, K. Cieslik-Boczula, J. Petrus, et al., Chemical structure of phenothiazines and their biological activity, Pharmacol. Rep. 64 (1) (2012) 16–23.
[47] J.G. Bernstein, Induction of obesity by psychotropic drugs, Ann. N. Y. Acad Sci. 499 (1987) 203–215.